Alpha-actinin of the chlorarchiniophyte *Bigelowiella natans*

Lars Backman

Department of Chemistry, Umeå University, Umeå, Sweden

ABSTRACT

The genome of the chlorarchiniophyte *Bigelowiella natans* codes for a protein annotated as an α-actinin-like protein. Analysis of the primary sequence indicate that this protein has the same domain structure as other α-actinins, a N-terminal actin-binding domain and a C-terminal calmodulin-like domain. These two domains are connected by a short rod domain, albeit long enough to form a single spectrin repeat. To analyse the functional properties of this protein, the full-length protein as well as the separate domains were cloned and isolated. Characerisation showed that the protein is capable of cross-linking actin filaments into dense bundles, probably due to dimer formation. Similar to human α-actinin, calcium-binding occurs to the most N-terminal EF-hand motif in the calmodulin-like C-terminal domain. The results indicate that this *Bigelowiella* protein is a proper α-actinin, with all common characteristics of a typical α-actinin.

INTRODUCTION

The cellular cytoskeleton is indispensable for any eukaryotic cell. This protein network, composed to varying degrees of actin filaments, intermediate filaments and microtubules, plays a role in all cellular events. The organisation and dynamics of the actin cytoskeleton is regulated by a variety of actin-binding proteins and other accessory proteins (*Dos Remedios et al., 2003*; *McGough, 1998*; *Winder & Ayscough, 2005*). One such accessory protein is α-actinin, that due to its ability to form antiparallel dimers is capable to cross-link actin filament into fibers or bundles as well as networks (*Foley & Young, 2014*; *Wachsstock, Schwarz & Pollard, 1993*).

α-actinin, like other members of the spectrin superfamily, is characterised by three structural domains: a N-terminal actin-binding domain, composed of two calponin homology domains, and a C-terminal calmodulin-like domain (*Broderick & Winder, 2005*; *Wasenius et al., 1987*). These domains are connected by a central rod domain consisting of spectrin-like repeats (*Blanchard, Ohanian & Critchley, 1989*; *Otey & Carpen, 2004*; *Sjöblom, Salmazo & Djinovic-Carugo, 2008*). Depending on the source of α-actinin, the rod domain contains one, two or four spectrin repeats. Vertebrate and invertebrate α-actinins have a rod with four repeats whereas α-actinin of fungal origin contains only two repeats (*Virel & Backman, 2004*; *Virel & Backman, 2007*). Some protozoa, like *Entamoeba histolytica* and *Encephalitozoon cuniculi* have a much shorter rod sequence, that may form a single repeat

but more likely fold into a coiled-coil region (*Virel & Backman, 2004*). Plants, algea and other photosynthesising organisms seem to lack α-actinin or α-actinin-like proteins. Therefore, it was surprising that the genome of the photosyntesising chlorarachniophyte *Bigelowiella natans* (*Neilson, Rangsrikitphoti & Durnford, 2017*) contains a gene that is annotated as a α-actinin-like protein (*Curtis et al., 2012*). No other members of the spectrin superfamily appears to be present in *Bigelowiella*.

Chlorarachniophytes are believed to have arisen through a secondary endosymbiosis when a green algae (a chlorophyte) was engulfed by a non-photosyntesising eukaryotic host (*Archibald et al., 2003*; *Curtis et al., 2012*; *Gould, Waller & McFadden, 2008*; *Neilson, Rangsrikitphoti & Durnford, 2017*; *Rogers et al., 2004*). Chlorarachniophytes have genetic material at four distinct locations; in the nucleus, mitochondria, plastid and nucleomorph, the remnant genome of the engulfed green algae (*Curtis et al., 2012*). Only a small number of genes (331) remains in the nucelomorph as most have been transferred to the nucleus or lost (*Gilson et al., 2006*). As present day green algaes lack α-actinin or α-actinin-like proteins, it is likely that the gene was already present in the genome of the host.

According to the JGI genome portal, the genome of *Bigelowiella* contain 610 gene models considered to be cytoskeletal. In addition to α-actinin, homologues of common actin-binding proteins are present; such as Arp2/3, filamin, gelsolin and many more. Recently, the evolution of key elements of the Chlorarachniophyte cytoskeleton in relation to the other Rhizaria phyla Foraminifera and Radiolariain were described (*Krabberød et al., 2017*). It was suggested that pseudopodia of Chlorarachniophytes rely on actin structures whereas those of Foraminifera and Radiolariain are dependent on microtubules. In vertebrates, α-actinin is involved in the attachment of actin filaments to membranes as well as in filopodia and lamellipodia formation (*Geiger et al., 1984*; *Hamill et al., 2015*; *Sobue & Kanda, 1989*; *Wehland, Osborn & Weber, 1979*). If the *Bigelowiella* α-actinin-like protein is a genuine α-actinin, it can be expected to have similar functions also in this organism. To investigate this, the *Bigelowiella* α-actinin-like protein and its structural domains were cloned, expressed in bacteria, isolated and characterized.

To my knowledge this is the first report on cloning, expression, isolation and characterisation of a *Bigelowiella* protein.

MATERIALS AND METHODS

Cloning, expression and purification

The sequence of *B. natans* α-actinin was obtained from Joint Genome Institute (JGI), accession number 89463. To facilitate subcloning, the N-terminal methionine was removed and BamHI and XhoI restriction sites were added to the 5′- and 3′-end, respectively. The final gene was synthesized and inserted in plasmid pUC57 by Genscript (Piscataway, NJ, USA). The resulting plasmid pUC57-BigN-ACTN was used to transform (by heat shock) competent *E. coli* TG1 cells. After over-night culture at 37 °C in Luria-Bertani medium containing 100 μM carbenicillin, plasmids were isolated using QIAprep Spin miniprep kit (Qiagen GmbH, Hilden, Germany). The α-actinin gene was excised by Bam HI and XhoI, gel purified and ligated into pET-TEV (a modified pET-19b vector) containing an N-terminal

Table 1 Domain assignments of *Bigelowiella natans* α-actinin by Superfamily, Smart and Pfam.

	Superfamily		Smart		Pfam	
	Region	*E*-value	Region	*E*-value	Region	*E*-value
Calponin homology domain	14–254	9.75e–56	26–131	5.82e–12	24–134	6.6e–16
Calponin homology domain	–	–	148–250	1.84e–23	146–256	9.0e–25
Spectrin repeat	274–384	3.7e—17	279–392	5.2e–2	–	–
EF-hand	372–488	9.45e–14	392–421	4.4e–6	392–420	2.6e–6
Ca2 +-insensitive EF-hand			459–520	1.44e–8	459–520	4.1e–9

Notes.

The amino acid sequence of *Bigelowiella natans* a-actinin was submitted to Superfamily (*Wilson et al., 2009*), Smart (*Letunic, Doerks & Bork, 2015*) and Pfam (*Finn et al., 2016*).

10xHis-tag and a TEV protease cleavage site. The resulting plasmid pTEV-BigN-ACTN was then used to transform (by heat shock) competent *E. coli* BL21(DE3).

Breakpoints for the structural domains of *B. natans* α-actinin-like protein were determined by alignment with other α-actinins as well as the database Superfamily (*Wilson et al., 2009*). When Smart (*Letunic, Doerks & Bork, 2015*) and Pfam (*Finn et al., 2016*) were interrogated with the amino acid sequence of *B. natans* α-actinin-like protein similar domain assignments were returned (Table 1). As shown in Fig. 1, the expressed full length *B. natans* α-actinin-like protein contains residues 2 to 524. The actin-binding domain (ABD) spans residues 2 to 260, the actin-binding domain with the rod domain (ABD-ROD) spans residues 2 to 372 and the rod domain (ROD) spans residues 257–392. Two constructs of the calmodulin-like domain (EF) were made, the longer construct (EF) contains residues 326 to 524 and the shorter (short-EF) begin at residue 370.

Plasmids expressing ABD, ABD-ROD, ROD and short-EF were created by mutagenesis of pTEV-BigN-ACTN. The gene fragment coding for EF was synthesized by Genscript, and ligated into pET-TEV, as described above, creating plasmid pTEV-BigN-EF.

Gene fragments were also inserted in pGEX-6P-2, adding glutathione S-transferse (GST) to the N-terminal instead of the His-tag. This resulted in plasmids pGEX-BigN-ABD, pGEX-BigN-ABD-ROD and pGEX-BigN-EF. To improve purification of expressed proteins, a His-tag (with 6 His residues) were added to the C-terminal. All constructs were sequenced (Eurofins MWG GmbH, Ebersberg, Germany; Genscript, Piscataway, NJ, USA) to control the fidelity of the final clones.

E. coli BL21(DE3) cells were transformed (by heat-shock) with the purified plasmids containing the different constructs. The transformed cells were cultured at 37 °C in Luria-Bertani medium containing 100 μM carbenicillin until an optical density of 0.6–0.8 at 600 nm was reached. Protein expression was induced by addition of isopropyl thio-β-D-galactoside to a final concentration of 0.5 mM and cells were grown overnight at 16 °C. Cells were harvested by centrifugation (29,000× g for 15 min), resuspended in 25 mM sodium phosphate buffer, pH 7.6, 150 mM NaCl and stored at −20 °C until the expressed protein was purified.

For purification, cells were thawed, polyethyleneimine was added to a final concentration of 0.05% and then lysed by sonication on ice. One-tenth volume of 10% Triton X-100 was added to the lysed cells. After 30 min incubation on ice, cell debris was removed
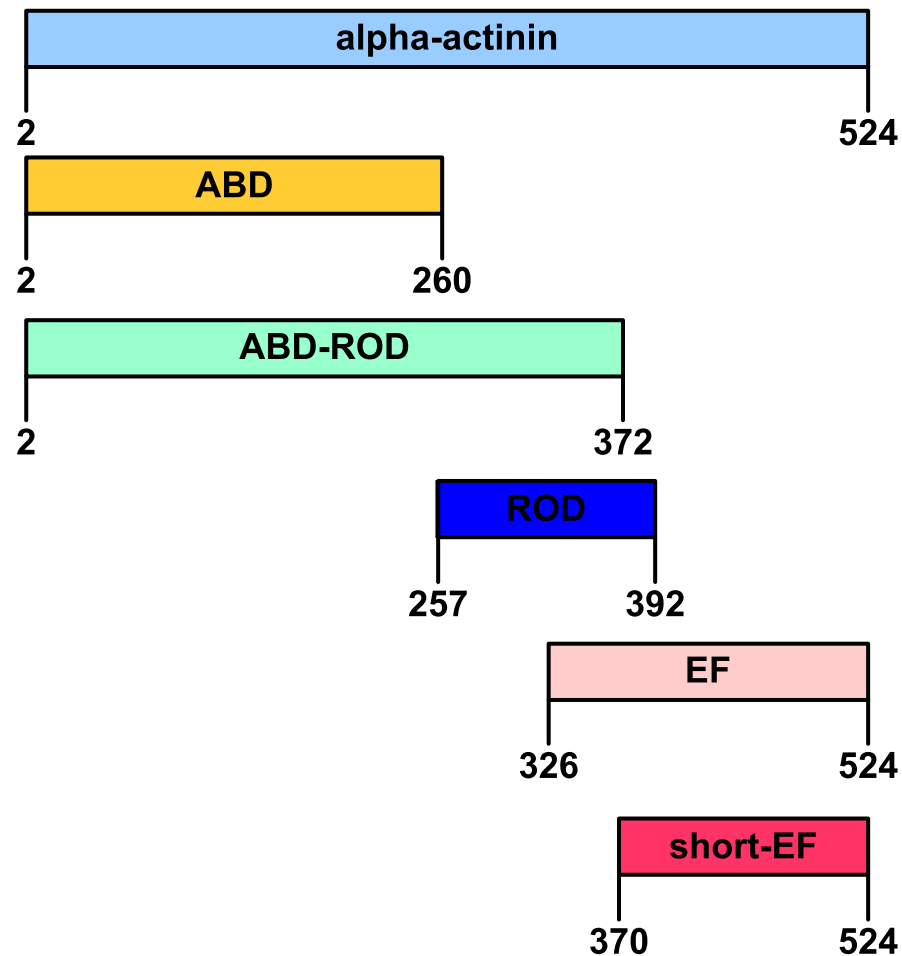
Figure 1 **Domain organization of *Bigelowiella* α-actinin-like protein.** The full-length protein contains a N-terminal actin-binding domain (ABD), a central rod domain (ROD), composed of one spectrin repeat and a C-terminal calmodulin-like domain (EF and shortEF) with EF-hand motifs. The first amino acid residue (methionine) was removed in all constructs.

Full-size ⊡ DOI: 10.7717/peerj.4288/fig-1

by centrifugation at 37,000× g for 20 min and the clarified supernatant loaded on an appropriate column.

Clarified supernatant of N-terminal His-tagged proteins were loaded on HiTrap^{TM} Chelating HP (GE Healthcare Bioscience AB, Sweden) columns charged with nickel. Unbound proteins were eluted with 25 mM sodium phosphate buffer, pH 7.6, 150 mM NaCl, 150 mM imidazole. Bound proteins were eluted with an imidazole gradient ranging from 150 to 500 mM imidazole in the same buffer. Imidazole was removed by gel filtration on HiPrep desalting columns (GE Healthcare Bioscience AB, Stockholm, Sweden). When required, Tobacco Etch Virus (TEV) protease (kindly provided by Dr. David S. Waugh) was used to hydrolyse the His-tag. The released 10xHis-tag and the 6xHis-tagged TEV protease were removed by affinity chromatography on a nickel-charged HiTrap^{TM} Chelating HP as before. To improve solubility, purified proteins were transferred into buffer TK (50

mM Tris, 200 mM KCl, pH 8.0) or buffer TKMG (50 mM Tris, 200 mM KCl, 10 mM β-mercaptoethanol, 10% glycerol, pH 8.0) by gel filtration on HiPrep desalting columns.

GST-tagged proteins were loaded on Glutathione-Sepharose columns (GE Healthcare Bioscience AB, Stockholm, Sweden). After unbound proteins had been eluted, bound proteins were eluted with 20–30 mM glutathione in 50 mM Tris, pH 8.0. The GST-tag was liberated by overnight incubation in the presence of protease C, obtained from the Protein Expert Platform (Umeå, Sweden). The GST-tagged moiety was removed by a second passage over the Glutathione-Sepharose. As before, purified proteins were transferred into buffer TK or TKMG by gel filtration on HiPrep desalting columns.

GST-free proteins with a C-terminal His-tag were purified further using affinity chromatography on a nickel-charged HiTrap^{TM} Chelating HP column as described above. The isolated protein was finally transferred into buffer TK or TKMG by gel filtration on a Hiprep 26/10 desalting column.

Protein concentration was determined from the absorbance at 280 nm using the molar absorptivity, as calculated from the amino acid sequence (using ProtParam at the ExPASy proteomics server). The purity of the expressed polypeptides was routinely determined under denaturating conditions by SDS-polyacrylamide gel electrophoresis (*Laemmli, 1970*).

Gel filtration

The propensity of purified polypeptides to form dimers or aggregates were determined by gel filtration on Toyopearl HW50-S 10/300 and Superdex 200 columns. Elution profiles were determined both in buffers TK and TKMG. Since the presence of glycerol affected the elution behaviour, a small volume of dissolved tryptophan was added to each sample as an internal standard and elution profiles were adjusted accordingly.

Ferritin (440 kDa) and bovine serum albumin (67 and 135 kDa) was used as references.

Actin co-sedimentation assay

Co-sedimentation was used to assay the ability of *Bigelowiella* α-actinin-like protein to cross-link actin. Actin was purified from rabbit skeletal muscle acetone powder as before (*Pardee & Spudich, 1982*; *Spudich & Watt, 1971*). Monomeric actin, in 5 mM Tris-HCl, pH 8.0, 0.2 mM $CaCl_2$ and 0.2 mM ATP, was polymerised by addition of KCl and $MgCl_2$ to final concentrations of 50 mM and 2 mM, respectively. Actin was allowed to polymerise for 60 min at room temperature. Polymerised actin was mixed with varying concentrations of full-length *Bigelowiella* α-actinin-like protein and incubated for 30 min at room temperature. After incubation, the reaction mixture was centrifuged at 13,000 rpm ($16,000\times$ g) for 15 min and supernatants and pellets were separated and analysed by SDS-PAGE (*Laemmli, 1970*). The amounts of actin in the pellets were quantified using Image Lab 5.2 (Bio-Rad laboratories).

Negative staining electron microscopy

The samples assayed by the co-sedimentation were also analysed by electron microscopy. Copper grids coated with formvar and carbon were prepared with Leica EM ACE200 carbon coating system. Grids were glow-discharged with Pelco easiGlow system (Ted Pella, Inc., Redding, CA, USA). 3.5 μl sample adsorbed for 2 min, washed twice in water and

immediately stained in 50 µl 1.5% uranyl acetate solution for 30 s. Samples were examined with Talos 120C (FEI, Eindhoven, The Netherlands) operating at 120 kV. Micrographs were acquired with a Ceta 16M CCD camera (FEI, Eindhoven, The Netherlands) using TEM Image & Analysis software ver. 4.15 (FEI, Eindhoven, The Netherlands).

Circular dichroism (CD) spectroscopy

Expressed polypeptides in buffer TK or TKMG with or without urea were analysed by CD spectroscopy using a Jasco J-810 spectrometer. Spectra between 200 and 260 nm were collected using 0.025 nm step-size and a scan speed of 50 nm per min, with a response time of 0.5 s and a bandwidth of 1 nm. Mean residue molar ellipticity was calculated from three accumulated spectra.

The temperature stability of expressed polypeptides was determined by the ellipticity at 222 nm. The thermal scan rate was 1 °C/min, with a data pitch of 0.2 °C, 2 nm bandwidth and 4 s response time.

Structure prediction

RaptorX (*Kallberg et al., 2012*; *Ma et al., 2013*) were used to predict the tertiary structure of separate domains. UCSF Chimera package was used to analyse structures and draw figures (*Pettersen et al., 2004*).

Calcium assay

^{45}Ca autoradiography was used to determine calcium binding as described (*Maruyama, Mikawa & Ebashi, 1984*). *Bigelowiella* α-actinin-like protein was blotted onto a PDVF membrane, wetted with 60 mM KCl, 5 mM $MgCl_2$, and 10 mM imidazole-HCl pH 6.8. The membrane was then incubated in the same solution containing ∼50 µM $^{45}CaCl_2$ (20.87 mCi/mg) for 1 h, rinsed with buffer and dried. Autoradiography was used to detect radioactive calcium.

RESULTS AND DISCUSSION

Cloning, expression and purification

The amino acid sequence of *Bigelowiella* α-actinin-like protein was retrieved from JGI. Based on this amino acid sequence corresponding DNA was synthesised. After subcloning into the expression vector (pET-TEV), this plasmid was used as template for preparing constructs of polypeptides used in this report.

All constructs expressed well and could be purified by metal chelating chromatography to reasonable purity. However, after removing the imidazole used to release the polypeptides from the metal chelating column, only the two EF peptides were soluble in salt-free buffer (50 mM Tris, pH 8.0). All other polypeptides as well as the full-length protein required addition of salt (NaCl and/or KCl) to reduce precipitation and aggregation. Although inclusion of 10% glycerol increased solubility of ABD, still a fraction, that increased with time, precipitated. Independent on the buffer systems tested, it has not been possible to find conditions to keep the polypeptides containing the rod domain, ABD-ROD and ROD, in solution.
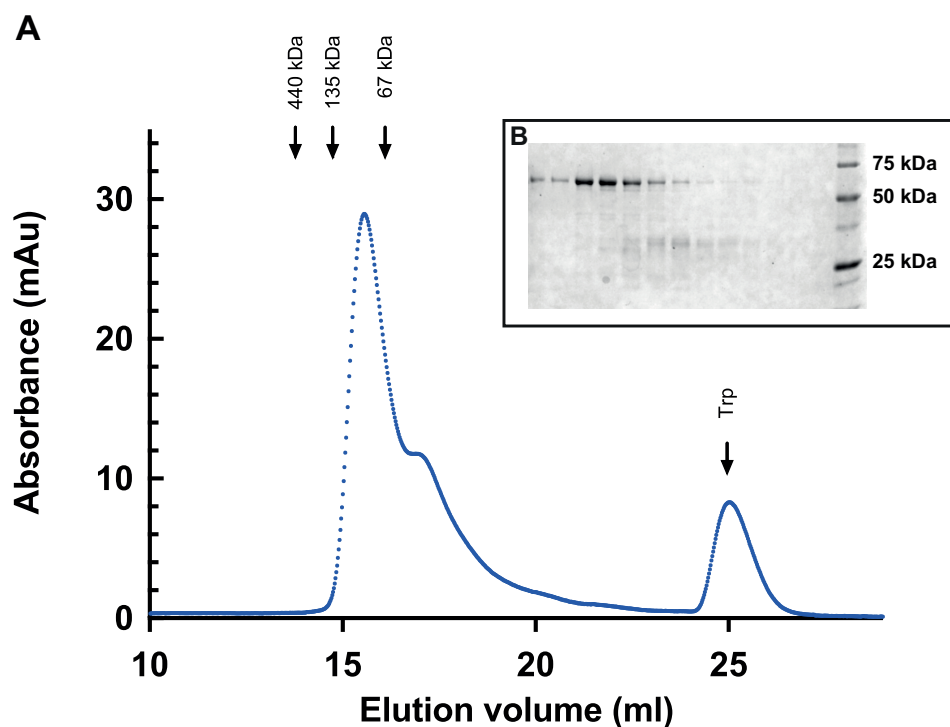
Figure 2 **Gel filtration of *Bigelowiella* α-actinin-like protein.** (A) The oligomeric state of the full-length α-actinin-like protein was determined by gel filtration on a Superdex 200 column, equilibrated with 50 mM Tris, 200 mM KCl, 10 mM β-mercaptoethanol, 10% glycerol, pH 8.0. 0.1 ml His-tagged protein was applied after centrifugation at 343,000× g for 30 min. The flow rate was 0.5 ml per min and absorbance at 280 was measure continuously. Ferritin (440 kDa), monomeric (67 kDa) and dimeric (135 kDa) bovine serum albumin were used as references. (B) Eluted fractions (0.5 ml) were collected and analysed by gel electrophoresis. From left to right, the stained gel shows protein content of fractions eluted between 14 and 20 ml.

Full-length a-actinin-like protein

After the full-length protein was released from the nickel-column and transferred into a imidazole-free buffer, the protein begun to form a visible precipitate. Inclusion of high concentration KCl together with glycerol and β-mercaptoethanol improved solubility but still a significant fraction was in an aggregated form.

By including a high-speed centrifugation step (343,000× g for 30 min) to remove aggregates before buffer change, no precipitation or aggregation was observed after change to the TKMG buffer. Although soluble, the amount of full-length protein that remained in solution decreased considerable and it degraded with time. When this material was applied on a Superdex 200 gel filtration column, the full-length protein eluted at a position between monomeric and dimeric bovine serum albumin, indicating that no higher oligomers or aggregates were present (Fig. 2A). The peak that eluted at ca 18 ml (seen as a shoulder in the figure), contained degradation products as seen in Fig. 2B.
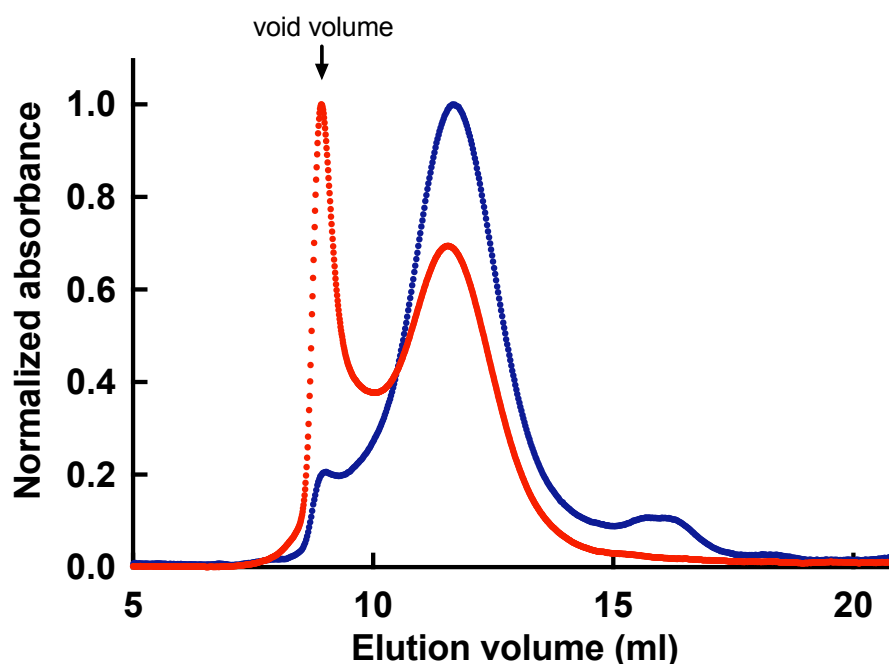
Figure 3 **Gel filtration of *Bigelowiella* actin-binding domain (ABD).** Aggregation was analysed by gel filtration on a Toyopearl HW50-S 10/300 column, equilibrated with 50 mM Tris, 200 mM KCl, 10 mM β-mercaptoethanol, 10% glycerol, pH 8.0. 0.1 ml His-tagged protein was applied directly after isolation (red) or after centrifugation at 343,000× g for 30 min (blue). The flow rate was 0.5 ml per min and absorbance at 280 nm was measured continuously. Void volume was determined from the elution pattern of ferritin (440 kDa). Data shown is representative of three independent experiments.

Full-size ☒ DOI: 10.7717/peerj.4288/fig-3

ABD

Similar to the full-length protein, also ABD displayed a propensity to precipitate when imidazole was removed. Although inclusion of 10% glycerol and β-mercaptoethanol increased solubility of ABD, still a fraction, that increased with time, precipitated. When aggregated material was removed by high-speed centrifugation (343,000× g for 30 min), monomeric ABD remained in the supernatant as determined by gel filtration. However, upon storage new aggregates formed as shown in Fig. 3.

ROD and ABD-ROD

It was not possible to find conditions to keep either of these polypeptides in solution after the initial purification step. Therefore, the properties of these two could not be determined reliably.

EF and short-EF

EF and short-EF could be purified to homogeneity even after cleavage of the N-terminal His-tag used for the initial purification step. Both EF-and short-EF were monomeric even in the absence of salt as determined by gel filtration.
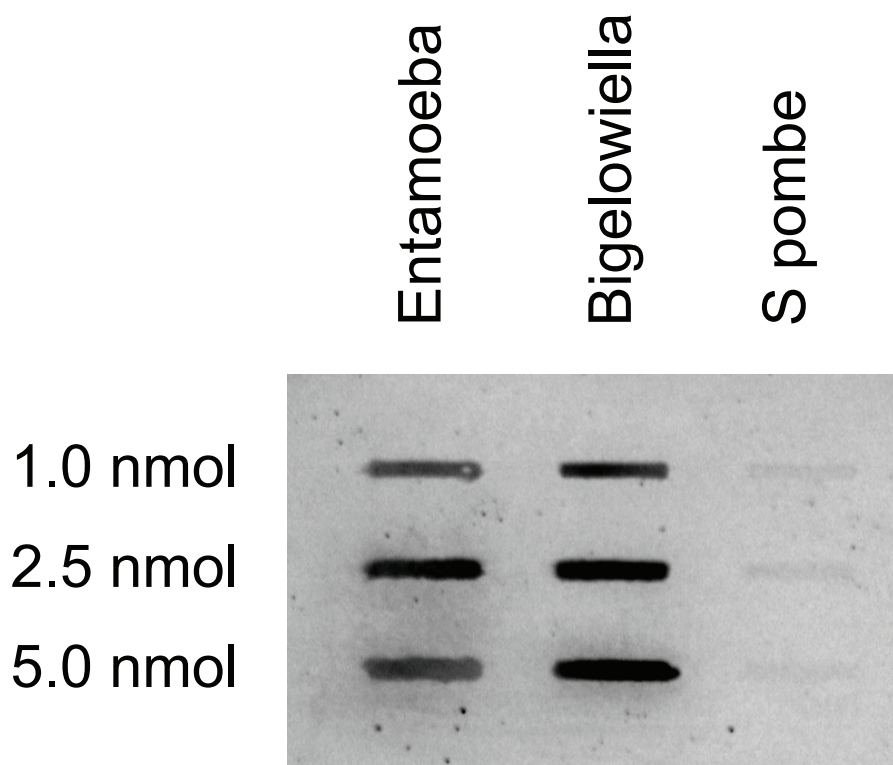
Figure 4 Calcium-binding properties of *Bigelowiella* α-actinin-like protein. *Bigelowiella* α-actinin-like protein was slot-blotted onto a PVDF membrane, together with *Entamoeba* α-actinin1 (positive control) and *S. pombe* α-actinin (negative control). Calcium-binding was probed by a calcium-overlay assay using ^{45}Ca.

Full-size 🖼 DOI: 10.7717/peerj.4288/fig-4

Calcium binding

Initially a ^{45}Ca-overlay assay showed that the *Bigelowiella* full-length α-actinin-like protein has affinity for calcium ions as shown in Fig. 4. The band intensity indicated that the binding affinity is similar to that of *Entamoeba histolytica* α-actinin2 (*Virel, Addario & Backman, 2007*). To analyse the calcium binding further a CD assay was used. The rationale being that ligand binding will increase the melting temperature of any protein, as the ligand must be dissociated before the protein unfolds and this require more energy, i.e., heat in this case.

   In all buffers tested, the CD spectra of EF were typical of a folded helical protein, with the typical negative peaks at 208 and 222 nm, independent on whether calcium ions were present or not (Fig. 5A). When comparing the melting traces in the absence and presence of calcium of EF and short-EF, only negligible differences were noticeable. It also was evident that the C-terminal domain was highly stable even at high temperatures. Therefore, in order to destabilize the protein, the denaturant urea was included in the CD measurements. As shown in Fig. 5B, increasing concentrations of urea led to increased unfolding of EF in the absence of calcium ions. However, in the presence of calcium ions, EF unfolded only partly. When the melting experiments were repeated in the presence of urea (∼3 M), it
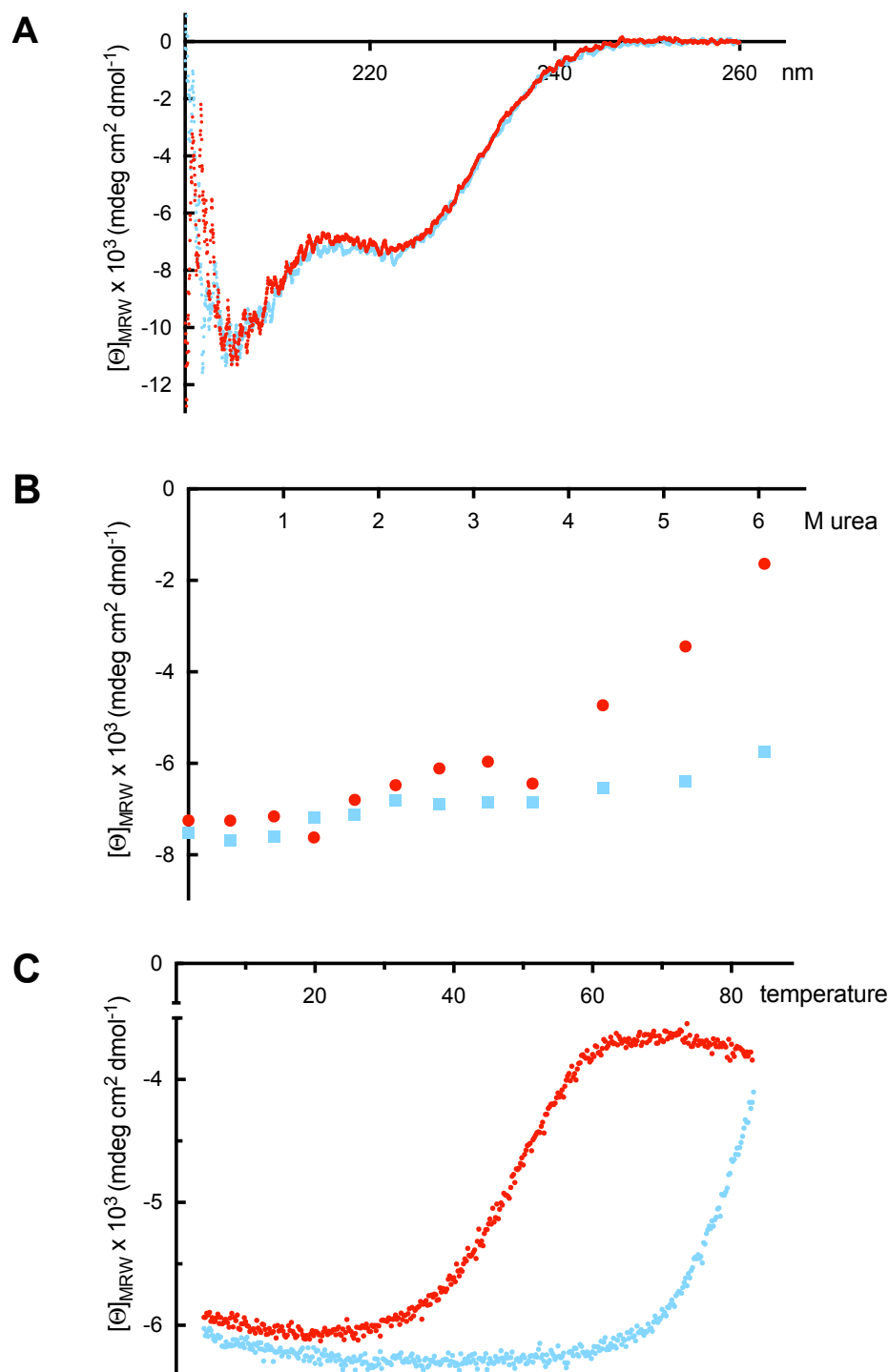
Figure 5 **Far UV-CD spectroscopy.** (A) Far UV-CD spectra of the calmodulin-like C-terminal of *Bigelowiella* in the absence (red) and presence (blue) 10 mM calcium ions. The mean residue molar ellipticity was determined from three accumulated scans between 200 and 260 nm at 20 °C, in 50 mM Tris, pH 8.0. (B) Urea unfolding of the calmodulin-like C-terminal in the absence (red) and presence (blue) of 10 mM calcium ions. The mean residue molar ellipiticy (continued on next page…)

Full-size DOI: 10.7717/peerj.4288/fig-5

Figure 5 (…continued)
at 222 nm was determined from three accumulated scans between 200 and 260 nm at 20 °C, in 50 mM Tris, pH 8.0. (C) The terminal stability of the calmodulin-like C-terminal in the absence (red) and presence (blue) of 10 mM calcium ions in 50 mM Tris, pH 8.0 and 2.9 M urea was determined from the mean residue molar ellipticity at 222 nm.

was evident that calcium stabilised EF; in the absence of calcium the melting transition was around 50 °C whereas addition of calcium increased the transition to around 80 °C or even higher (Fig. 5C). The same results were obtained for shortEF (not shown). These results indicate that the calcium affinity is associated with the calmodulin-like C-terminal and the EF-hand motifs.

Superfamily (Wilson et al., 2009) identified residues 372–488 as an EF-hand domain with a very low E-value (4.84×10^{-15}). Pfam (Finn et al., 2016) and Smart (Letunic, Doerks & Bork, 2015) identified residues 392–420 as an active EF-hand domain (E-values: 2.6×10^{-6} and 6.54×10^{-6}, respectively) and residues 459–520 as a calcium-insensitive EF-hand domain (E-values: 4.1×10^{-9} and 1.44×10^{-8}). Inspection and alignment to other EF-hand domains and the consensus sequence indicated that only the first EF-hand motif has proper residues in the positions involved in coordinating the calcium ion as Fig. 6 shows. The other three motifs lack one or more of the residues believed to be required for calcium binding.

Actin binding

The ability of α-actinins to form antiparallel dimers creates binding sites for actin at each end of the dimer, that allows the dimer to cross-link or bundle actin filaments. It is generally believed that the rod domain is required for dimer formation and that the calponin homology domains constitute the binding site for actin. If correct also for the Bigelowiella α-actinin-like protein, ABD and ABD-ROD would bind actin filaments but only ABD-ROD would cross-link or bundle filaments, in addition to the full-length protein.

The rationale of the co-sedimentaion assay is that cross-linked or bundled actin filaments are pelleted by a low-speed centrifugation whereas any actin binder would only be pelleted with actin filaments by a high-speed centrifugation. Therefore, increasing concentrations of the *Bigelowiella* α-actinin-like protein were incubated with actin filaments before a low-speed centrifugation. As seen in Fig. 7A, in the absence of the α-actinin-like protein only a very small amount of actin was pelleted. On the other hand, in the presence of increasing concentrations of the full-length α-actinin-like protein, increasing amounts of both proteins were found in the pelleted material, indicating cross-linking or bundling of actin. Quantification indicated that a ratio of one cross-linker to two actin monomers were enough for maximal cross-linking (Fig. 7B), very similar to the behaviour of *Entamoeba histolytica* α-actinin (Virel, Addario & Backman, 2007). As gel filtration indicated that no higher oligomers were present, these results clearly indicate that the α-actinin-like protein dimerises.

This was corroborated by transmission electron microscopy. In the presence of the *Bigelowiella* protein actin filaments form networks and bundles, not seen in its absence (Fig. 8).

		Ca^{2+} binding loop			linker

EF-hand motif 1

Canonical sequence		En**nn**n	X*Y*ZGyIx**z	n**nn**n	
calmodulin	ADQLTEEQIA	EFKEAFSLF	DKDGDGTITTKE	LGTVMRSL	GQNPTEA
troponin C	TDQQAEARSYLSEEMIA	EFKAAFDMF	DADGGGDISVKE	LGTVMRML	GQTPTKE
Human1	ENQILTRDAKGISQEQMN	EFRASFNHF	DRDHSGTLGPEE	FKACLISL	GYDIGNDPQGEA
Human2	ETQILTRDAKGITQEQMN	EFRASFNHF	DRRKNGLMDHED	FRACLISM	GYDLGEA
Human3	ENQVLTRDAKGLSQEQLN	EFRASFNHF	DRKRNGMMEPDD	FRACLISM	GYDLGEV
Human4	ENQILTRDAKGISQEQMQ	EFRASFNHF	DKDHGGALGPEE	FKACLISL	GYDVENDRQGEA
Entamoeba	GSSSGVTAEQMQ	EFKQSFDAF	DGNHDGILDKLE	FRSCLSSM	GLIDIDFTGGEDA
Bigelowiella	HELQQAEAKYKATPEQLQ	EFEESFNHF	DDNSDGTLNRDE	FKAALSAL	GIAFKDDQ

EF-hand motif 2

Canonical sequence		En**nn**n	X*Y*ZGyIx**z	n**nn**n	
calmodulin		ELQDMINEV	DADGNGTIDFPE	FLTMMARK	MKDTDSEE
troponin C		ELDAIIEEV	DEDGSGTIDFEE	FLVMMVRQ	MKEDAKGKSEE
Human1		EFARIMSIV	DPNRLGVVTFQA	FIDFMSRE	TADTDTAD
Human2		EFARIMTLV	DPNGQGTVTFQS	FIDFMTRE	TADTDTAE
Human3		EFARIMTMV	DPNAAGVVTFQA	FIDFMTRE	TAETDTTE
Human4		EFNRIMSLV	DPNHSGLVTFQA	FIDFMSRE	TTDTDTAD
Entamoeba		QYDAIYNNV	TKGENG-VSFDN	YVQYMKEK	NDENPSPE
Bigelowiella		DFEKVFKKV	GEGAET-ISKDL	YMKYMKAI	SEDKGTAE

EF-hand motif 3

Canonical sequence		En**nn**n	X*Y*ZGyIx**z	n**nn**n	
calmodulin		EIREAFRVF	DKDGNGYISAAE	LRHVMTNL	GEKLTDE
troponin C		ELAECFRIF	DRNADGYIDAEE	LAEIFRAS	GEHVTDE
Human1		QVMASFKIL	AGDKN-YITMDE	LRRELPPD	QA
Human2		QVIASFRIL	ASDKP-YILAEE	LRRELPPD	QA
Human3		QVVASFKIL	AGDKN-YITPEE	LRRELPAK	QA
Human4		QVIASFKVL	AGDKN-FITAEE	LRRELPPD	QA
Entamoeba		QLNEIFSTI	AAGKD-SITETD	MQKAGMSA	EQI
Bigelowiella		EQVETSFMA	LADGKSYITAEQ	LEG-LPEE	DK

EF-hand motif 4

Canonical sequence		En**nn**n	X*Y*Z---GyIx**z	n**nn**n	
calmodulin		EVDEMIREA	DIDGD---GQVNYEE	FVQMMTAK	
troponin C		EIESLMKDG	DKNND---GRIDFDE	FLKMMEGV	Q
Human1		EYCIARMAP	YTGPDSVPGALDYMS	FSTALYGE	SDL
Human2		QYCIKRMPA	YSGPGSVPGALDYAA	FSSALYGE	SDL
Human3		EYCIRRMVP	YKGSGAPAGALDYVA	FSSALYGE	SDL
Human4		EYCIARMAP	YQGPDAVPGALDYKS	FSTALYGE	SDL
Entamoeba		EYVKANL-P	QKG-D---GY-DYAA	WVKTN	
Bigelowiella		QFLQDNMEA	GEEK----GAFNYKQ	LVQKSFVD	EAE

Figure 6 **Calcium binding motifs.** The sequence of the calmodulin-like C-terminal domain of *Bigelowiella* a-actinin-like protein was aligned with C-terminal domains of other α-actinins as well as with the canonical sequence. In the calcium binding loop residues at positions X, Y, Z, y, x and z coordinate the calcium ion, generally by side chain oxygens. The residue at position y coordinates the calcium ion through the backbone carbonyl oxygen. In the canonical sequence: E, glutamate; G, glycine; I, isoleucine, leucine or valine; n, hydrophobic residue; *, any residue. Based on the Prosite PS00018 pattern: D-W-[DNS]-ILVFYW-[DENSTG]-[DNQGHRK]-GP-[LIVMC]-[DENQSTAGC]-x(2)-[DE]-[LIVNFYM], red indicates a residue present in active EF-hand motifs, whereas blue indicates a residue not commonly found in this position of the calcium binding loop.
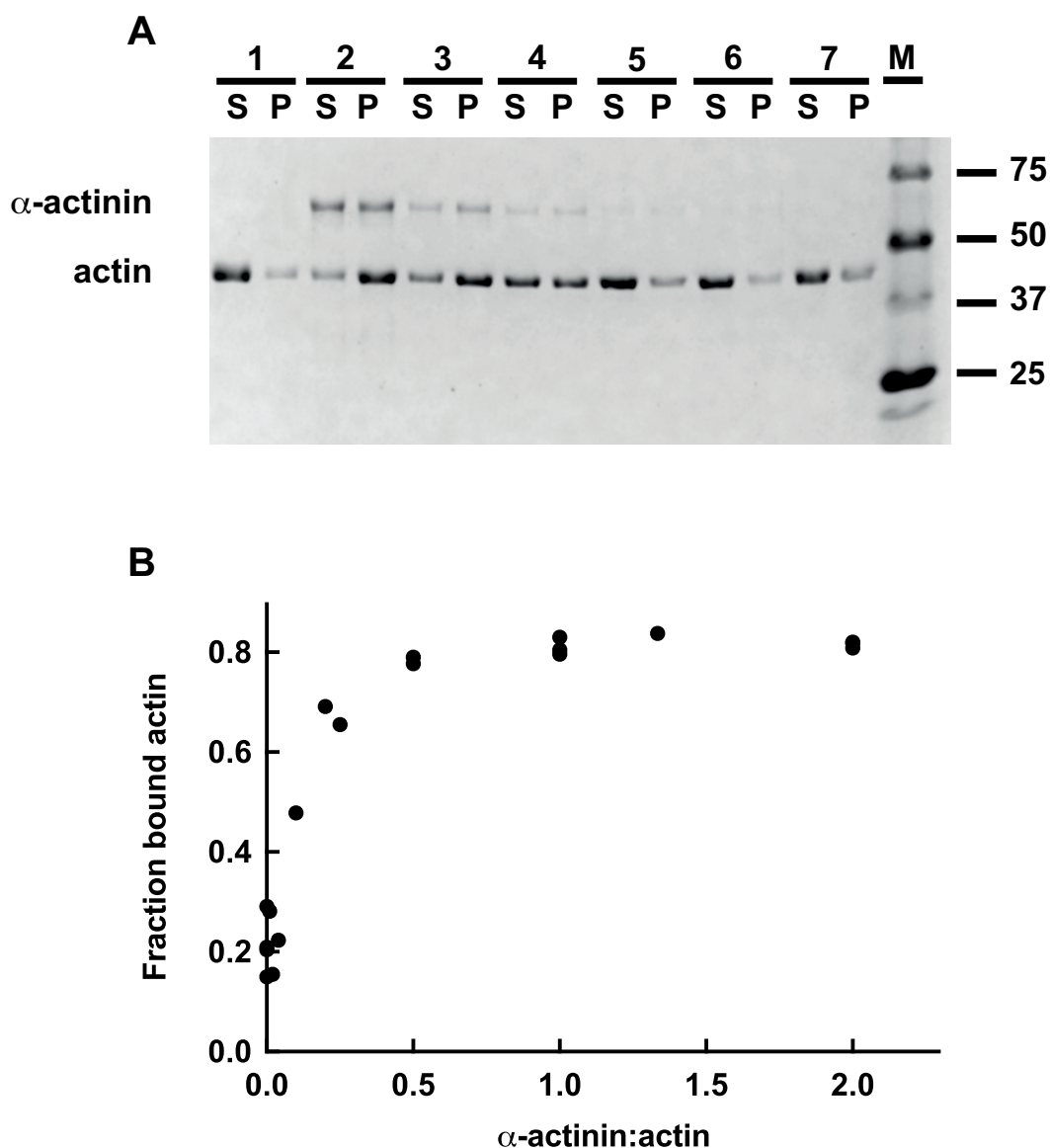
Full-size 🖾 DOI: 10.7717/peerj.4288/fig-6

Figure 7 **Low speed actin co-sedimentation assay.** (A) *Bigelowiella* α-actinin-like protein and polymerised actin were incubated for 30 min separately or together at different concentrations. After 30 min at room temperature, the samples were centrifuged (13,000 rpm, 15 min) and supernatant (S) and pellet (P) were separated on 10% SDS-PAGE and visualized by Coomassie Blue staining. Lane 1: 5 μM actin; lanes 2–7: 5 μM actin together with 2.5, 1, 0.5, 0.2, 0.1 and 0.05 μM α-actinin-like protein; M: protein ladder. Data shown are representative of three experiments. (B) The fraction of actin pelleted by the presence of full-length α-actinin-like protein was quantified by analysis of stained gels using Image Lab.

Full-size 🖾 DOI: 10.7717/peerj.4288/fig-7

Due to the propensity of ABD and ABD-ROD to aggregate and precipitate it was not feasible to investigate their binding further, as even a low-speed spin pelleted most of the ABD-ROD. Likewise, nearly all ABD was found in the pellet after a high-speed centrifugation.
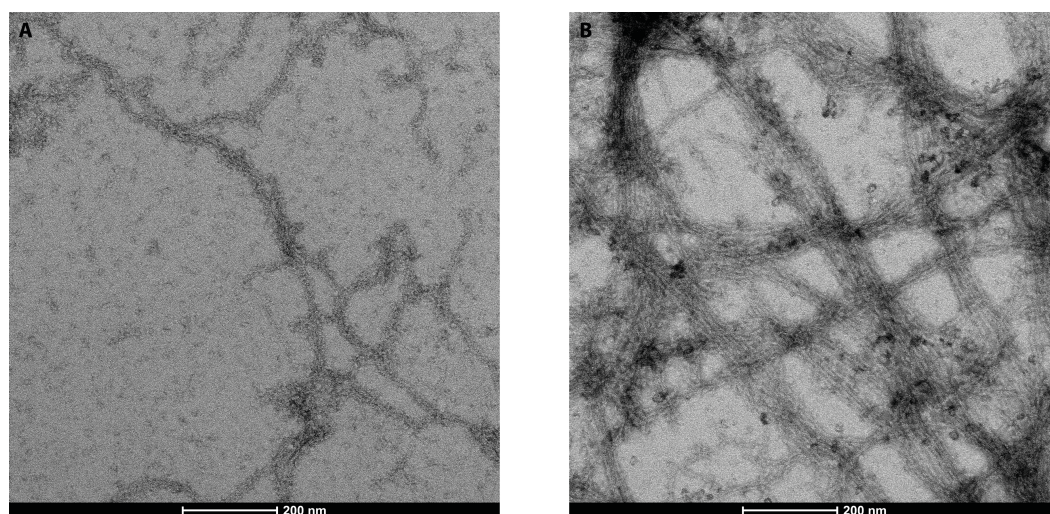
Figure 8 Electron transmission microcopy. 5.0 μM actin was incubated alone (A) or with 1.25 μM *Bigelowiella* a-actinin-like protein (B) as before, added to grids and negatively stained with uranylacetate. Bar: 200 nm.

Full-size 🖻 DOI: 10.7717/peerj.4288/fig-8

Table 2 Validation scores for the predicted structures using Protein Structure Validation Software.

	ABD		ROD		EF		short EF	
	Mean score	Z-score	Mean score	Z-score	Mean score	Z-score	Mean score	Z-score
Structure quality factors								
Procheck G-factor (phi/psi only)	0.21	1.14	0.57	2.56	0.07	0.59	0.02	0.39
Procheck G-factor (all dihedral angles)	0.05	0.30	0.35	2.07	−0.04	−0.24	−0.01	−0.06
Verify3D	0.45	−0.16	0.31	−2.41	0.24	−3.53	0.30	−2.57
ProsaII	0.55	−0.41	0.78	0.54			0.82	0.70
MolProbity clashscore	124.94	−19.91	83.22	−12.76	119.69	−19.01	96.20	−14.98
Ramachandran plot summary from procheck								
Most favoured regions	89.9%		91.1%		86.5%		88.9%	
Additionally allowed regions	7.9%		8.1%		10.7%		9.7%	
Generously allowed regions	0.9%		0.8%		2.2%		0.0%	
Disallowed regions	1.3%		0.0%		0.6%		1.4%	
Ramachandran plot statistics from Richardson's lab								
Most favoured regions	95.2%		94.9%		93.9%		92.3%	
Allowed regions	2.4%		4.4%		4.6%		5.8%	
Disallowed regions	2.4%		0.7%		1.5%		1.9%	

Homology modelling

The amino acid sequences of ABD, ROD, EF and short EF were submitted to the web server RaptorX for structure predictions (*Kallberg et al., 2012*; *Ma et al., 2013*). The qualities of the predicted structures were validated using the Protein Structure Validation Software suite (*Bhattacharya, Tejero & Montelione, 2007*). Table 2 shows validation scores for the
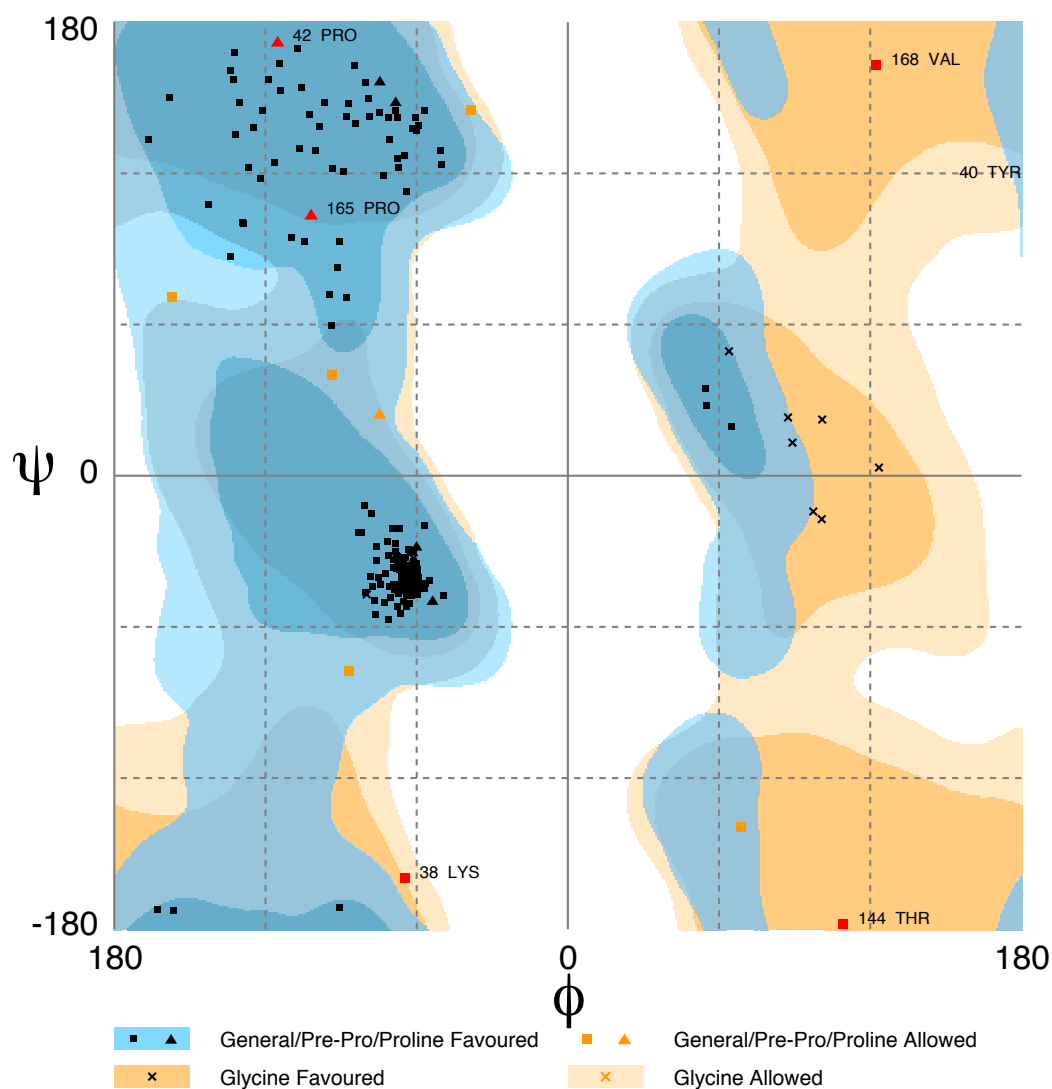
Figure 9 Ramachandran plot of the actin-binding domain (ABD) of *Bigelowiella* α-actinin-like protein. The quality of the predicted structure of ABD was analysed by Rampage. Six residues (Lys38, Tyr40, Pro42, Thr144, Pro 165 and Val168) were found in disallowed regions.

Full-size 🖼 DOI: 10.7717/peerj.4288/fig-9

predicted structures. The scores indicate that the structures are reasonable accurate, with only a few residues in disallowed regions. This is illustrated in Fig. 9, by the Ramachandran plot of the ABD model which places six residues in disallowed regions (Lys38, Val40, Pro42, Thr14, Pro165 and Val168).

One of the templates used in the homology modelling of ABD, was the actin-binding domain of *Schizosaccharomyces pombe* α-actinin. Although the sequence of *Bigelowiella* ABD is only ca 39% identical to the ABD of *S pombe* (pdb: 5bvr), the DaliLite server (*Hasegawa & Holm, 2009*) returns a very high Z-score of 32.5 and a low root mean deviation value of 1.0 Å. When the Dali server was interrogated with *Bigelowiella* ABD as query structure, several structures with very high Z-scores and low rmsd values were
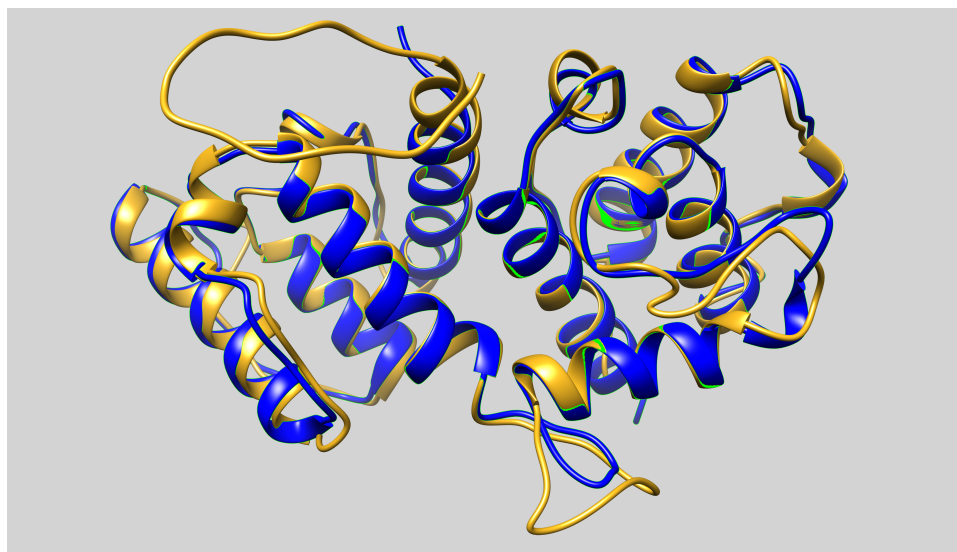
Figure 10 **The actin-binding domain.** The predicted structure of actin-binding domain (ABD) of *Bigelowiella* α-actinin-like protein (goldenrod) was superimposed with the crystal structure of *S. pombe* α-actinin ABD (blue, pdb: 5bvr).

returned. The returned *Z*-score of the actin-binding domain of human α-actinin3 (pdb: 1wku) and α-actinin4 (pdb: 2r0o) were 33.8 and 33.5, respectively, and the rmsd were in both cases 1.0 Å. The major structural differences between the predicted structure of *Bigelowiella* ABD and determined structure of *S pombe* ABD are located to loops connecting the helices (Fig. 10).

The predicted structure of the *Bigelowiella* ROD domain is similar to all other determined spectrin repeats although the sequence identity in general is low (Fig. 11). When the amino acid sequence is compared to one of the templates used in the prediction, the rod domain of human α-actinin (pdb: 1hci), the sequence identity of either of the four repeats is around 20% or less (Fig. 12). Still the *Z*-scores and rmsd values range from 11.7 to 14.3 and 1.6 to 2.5, respectively, as determined by the DaliLite server.

Spectrin repeats are found in several cytoskeletal proteins, such as spectrin, dystrophin and plectin as well as α-actinins. The common structure of a spectrin repeat is a three-helix bundle. These repeats are defined by a tryptophan residue at position 17 in the first helix and a leucine residue two residues from the C-terminal end of the third helix. This tryptophan is believed to be essential for folding and stability of the triple-helix motif (*Kusunoki, MacDonald & Mondragon, 2004*; *MacDonald et al., 1994*; *Pantazatos & MacDonald, 1997*). Interestingly, such a tryptophan is present in the predicted ROD structure (Fig. 11).

The central domain of *Entamoeba histolytica* α-actinin1 is also short, spanning ca 120 residues, and probably does not form a spectrin repeat but rather a coiled structure (*Virel & Backman, 2006*). Since *Entamoeba* α-actinin1, like *Bigelowiella* α-actinin, cross-links actin filaments these α-actinins presumably dimerises by homotypic interactions between the central domain whether it is a spectrin repeat or not. In contrast, in α-actinins with
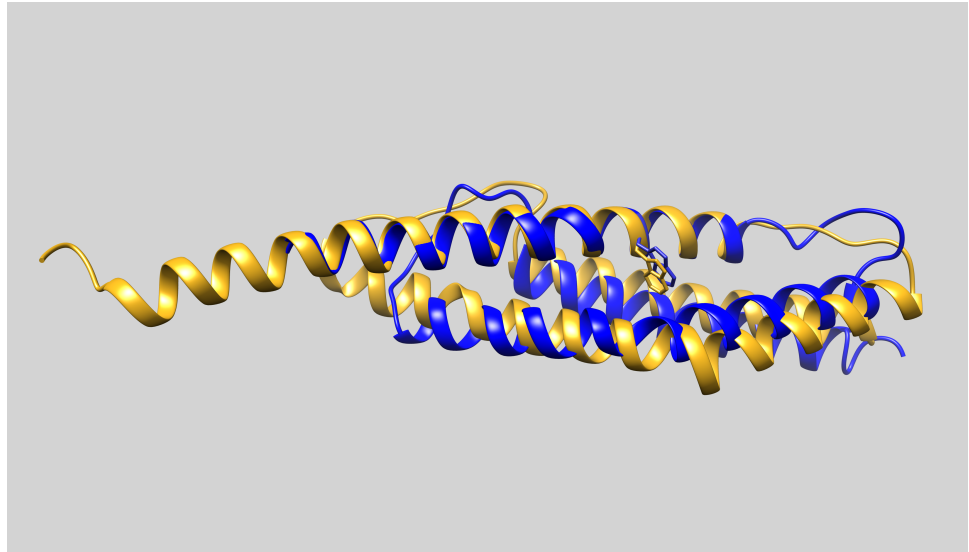
Figure 11 The rod domain. The model of the rod domain of *Bigelowiella* α-actinin-like protein (golden-rod) was superimposed with the first spectrin repeat of human α-actinin2 (blue, pdb: 1hci). The characteristic tryptophan important for the stability of spectrin repeats is shown explicitly.

Full-size ⬛ DOI: 10.7717/peerj.4288/fig-11


```
              10        20        30        40        50        60        70
              |         |         |         |         |         |         |
Human2        AEQAETAANRICKVLAVNQENERLMEEYERLASELLEWIRRTIPWLENRTPEKTMQAMQKKLEDFRDYRR
Bigelowiella  LGEKQAAVRRVKQFIAFQRQIWEQQNDYKARAETLMKWADGKISEYTKCDLGDTKEEVETGRSKLKEYLK
Entamoeba2    NDQVEKAGKRAGNFLDFLRATEGMVHDYEQRAQALKENIEAAINKMNGVEPSDEYHQVKEQINETKNYRK
Pombe         LDKVETAARRVERFTEVLMSTHDMKIDYESRMKRLLGSIARMQEYWHTVQFENNYTDVKSHSNNFAKFKA
Entamoeba1    REEQERKQKEEQERLAREEQERLAREEQERLAREEQERLAREEQERKQKEEQERLAREEQERKQREEQER

              80        90        100       110       120       130
              |         |         |         |         |         |
Human2        KHKPPKVQEKCQLEINFNTLQTKLRISNRPAFMPSEGKMVSDIAGAWQRLEQAEKGYEEWLLNEIR
Bigelowiella  SVKPGKAVEKMDIESLYGEIQANLRINNRSPYCPPGSCAPNSLDSKWHELQQAEAKYKATPEQLQE
Entamoeba2    GDKRAFIKEQGDLATLFGQINSKLRGMKRPVYVAPEGLDPKSLEGYIANISEAERALRSKLNTAMR
Pombe         TEKREWVKEKIDLESLLGTIQTNLKTYQLRKYEPPAGLKIVDLERQWKDFLSEEANQSKLINTHMR
Entamoeba1    LNQQQPTSQQLTFFSVQAAADAWILQNIQAAYAQDPTIQFQWWYPLVQNLSANDFRELQDWFKKID
```

Figure 12 Alignment of the rod domain. The sequences of human (accession: NM_001130004), *Entamoeba histolytica* (accessions: AF208390 and XM_648191) and *Schizosaccharomyces pombe* (accession: NM_001019718) α-actinins were aligned with *Bigelowiella natans* α-actinin using Multalin (*Corpet, 1988*). Shaded regions are predicted by J Pred to be helical (*Drozdetskiy et al., 2015*).

Full-size ⬛ DOI: 10.7717/peerj.4288/fig-12

four spectrin repeats dimerization occurs by heterotypic interactions between the first and last and between the second and third spectrin repeat (*Djinovic-Carugo et al., 1999*; *Flood et al., 1995*; *Flood et al., 1997*).

When the predicted structure of shortEF was submitted to the Dali server, the returned top-scorer was the C-terminal calmodulin-like domain of *Entamoeba histolytica* α-actinin2 (pdb: 2m7l), with a *Z*-score of 18.0 and a rmsd of 0.9 Å (Fig. 13). The same structure was also found when EF was used as query.
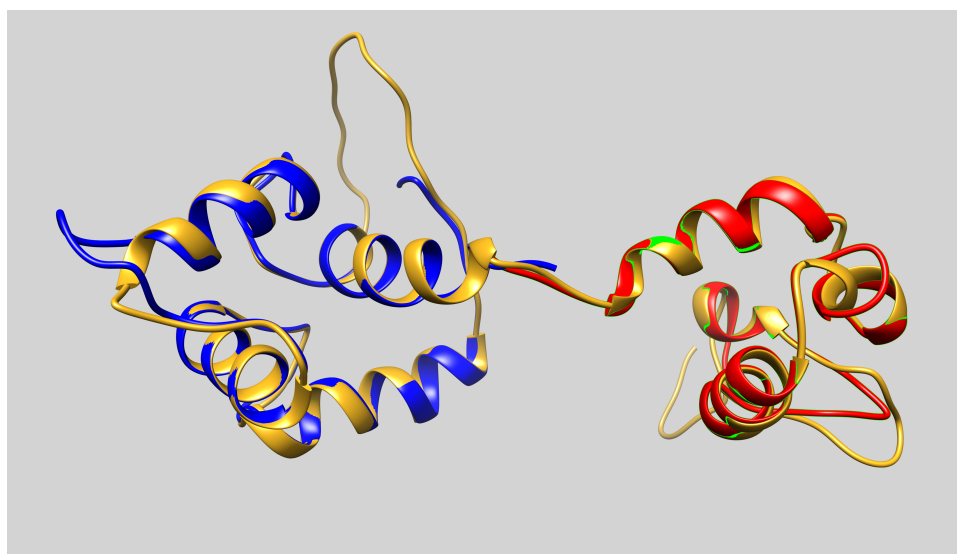
Figure 13 The calmodulin-like C-terminal domains. The predicted structure of the calmodulin-like C-terminal domain (goldenrod) of *Bigelowiella* α-actinin-like protein was superimposed with the N-terminal (blue) and C-terminal (red) halves, respectively, of *E. histolytica* (pdb: 2m7l).

Full-size 🖾 DOI: 10.7717/peerj.4288/fig-13

CONCLUSION

I have cloned, expressed, isolated and characterized a *Bigelowiella* protein with all characteristics of an α-actinin. Structural and functional annotation by Superfamily (*Wilson et al., 2009*) identified a N-terminal calponin-homology domain, a C-terminal EF-hand domain and a single spectrin repeat between the terminals. Direct binding assays as well as transmission electron microscopy showed that the protein cross-links actin filaments into dense bundles. Although experiments to localize the actin-binding site were impossible due to the protein's propensity to precipitate, it is very likely that binding occurs to the N-terminal and the calponin homology domain, as in other α-actinins. Since both the full-length protein and the two C-terminal constructs bound calcium, it is apparent that the calcium-affinity is due to one (or more) of the EF-hand motifs. Since only the first EF-hand motif has the proper residues required for coordination of the calcium ion, it is probable that this motif also is responsible for the calcium binding, similar to the calmodulin-like domain of human α-actinin1 (*Drmota Prebil et al., 2016*).

Although some residues occurred in the disallowed regions of the Ramachandran plots, the quality of the predicted structures were high and very similar to known α-actinin domain structures. Major differences in all domain models were located to loop regions.

Based on the experimental results as well as on the homology modelling, is it evident that this *Bigelowiella* protein is a genuine α-actinin.

It has been suggested that the rod domain in α-actinin may function as a platform coordinating interactions with structural and signalling proteins (*Djinovic-Carugo et al., 2002*). Since the rod domain in *Bigelowiella* α-actinin spans only one spectrin repeat, in contrast to four repeats in α-actinins from multicellular organisms, less surface area

is available for such a function. Alpha-actinin has been implicated in several cellular functions, such as cytokinesis (*Fujiwara, Porter & Pollard, 1978*; *Li et al., 2016*), movement (*Matsudaira, 1994*; *Meacci et al., 2016*; *Sobue & Kanda, 1989*) and contraction (*Gautel & Djinovic-Carugo, 2016*; *Maruyama & Ebashi, 1965*). Whether *Bigelowiella* α-actinin has similar functions requires further studies.

ACKNOWLEDGEMENTS

ADDITIONAL INFORMATION AND DECLARATIONS

Competing Interests
The author declares there are no competing interests.

Author Contributions
- Lars Backman conceived and designed the experiments, performed the experiments, analyzed the data, contributed reagents/materials/analysis tools, wrote the paper, prepared figures and/or tables, reviewed drafts of the paper.

Data Availability
The following information was supplied regarding data availability:
The pdb models are provided as Supplemental Files.

Supplemental Information
Supplemental information for this article can be found online at http://dx.doi.org/10.7717/peerj.4288#supplemental-information.

REFERENCES

Archibald JM, Rogers MB, Toop M, Ishida K, Keeling PJ. 2003. Lateral gene transfer and the evolution of plastid-targeted proteins in the secondary plastid-containing alga *Bigelowiella natans*. *Proceedings of the National Academy of Sciences of the United States of America* **100**:7678–7683 DOI 10.1073/pnas.1230951100.

Bhattacharya A, Tejero R, Montelione GT. 2007. Evaluating protein structures determined by structural genomics consortia. *Proteins: Structure, Function, and Bioinformatics* **66**:778–795 DOI 10.1002/prot.21165.

Blanchard A, Ohanian V, Critchley D. 1989. The structure and function of α-actinin. *Journal of Muscle Research and Cell Motility* **10**:280–289 DOI 10.1007/BF01758424.

Broderick MJ, Winder SJ. 2005. Spectrin, a-actinin, and dystrophin. *Advances in Protein Chemistry* **70**:203–246 DOI 10.1016/S0065-3233(05)70007-3.

Corpet F. 1988. Multiple sequence alignment with hierarchical clustering. *Nucleic Acids Research* **16**:10881–10890.

Curtis BA, Tanifuji G, Burki F, Gruber A, Irimia M, Maruyama S, Arias MC, Ball SG, Gile GH, Hirakawa Y, Hopkins JF, Kuo A, Rensing SA, Schmutz J, Symeonidi A, Elias M, Eveleigh RJ, Herman EK, Klute MJ, Nakayama T, Obornik M, Reyes-Prieto A, Armbrust EV, Aves SJ, Beiko RG, Coutinho P, Dacks JB, Durnford DG, Fast NM, Green BR, Grisdale CJ, Hempel F, Henrissat B, Hoppner MP, Ishida K, Kim E, Koreny L, Kroth PG, Liu Y, Malik SB, Maier UG, McRose D, Mock T, Neilson JA, Onodera NT, Poole AM, Pritham EJ, Richards TA, Rocap G, Roy SW, Sarai C, Schaack S, Shirato S, Slamovits CH, Spencer DF, Suzuki S, Worden AZ, Zauner S, Barry K, Bell C, Bharti AK, Crow JA, Grimwood J, Kramer R, Lindquist E, Lucas S, Salamov A, McFadden GI, Lane CE, Keeling PJ, Gray MW, Grigoriev IV, Archibald JM. 2012. Algal genomes reveal evolutionary mosaicism and the fate of nucleomorphs. *Nature* **492**:59–65 DOI 10.1038/nature11681.

Djinovic-Carugo K, Gautel M, Ylanne J, Young P. 2002. The spectrin repeat: a structural platform for cytoskeletal protein assemblies. *FEBS Letters* **513**:119–123 DOI 10.1016/S0014-5793(01)03304-X.

Djinovic-Carugo K, Young P, Gautel M, Saraste M. 1999. Structure of the a-actinin rod: molecular basis for cross-linking of actin filaments. *Cell* **98**:537–546 DOI 10.1016/S0092-8674(00)81981-9.

Dos Remedios CG, Chhabra D, Kekic M, Dedova IV, Tsubakihara M, Berry DA, Nosworthy NJ. 2003. Actin binding proteins: regulation of cytoskeletal microfilaments. *Physiological Reviews* **83**:433–473 DOI 10.1152/physrev.00026.2002.

Drmota Prebil S, Slapsak U, Pavsic M, Ilc G, Puz V, De Almeida Ribeiro E, Anrather D, Hartl M, Backman L, Plavec J, Lenarcic B, Djinovic-Carugo K. 2016. Structure and calcium-binding studies of calmodulin-like domain of human non-muscle alpha-actinin-1. *Scientific Reports* **6**:27383 DOI 10.1038/srep27383.

Drozdetskiy A, Cole C, Procter J, Barton GJ. 2015. JPred4: a protein secondary structure prediction server. *Nucleic Acids Research* **43**:W389–W394 DOI 10.1093/nar/gkv332.

Finn RD, Coggill P, Eberhardt RY, Eddy SR, Mistry J, Mitchell AL, Potter SC, Punta M, Qureshi M, Sangrador-Vegas A, Salazar GA, Tate J, Bateman A. 2016. The Pfam protein families database: towards a more sustainable future. *Nucleic Acids Research* **44**:D279–D285 DOI 10.1093/nar/gkv1344.

Flood G, Kahana E, Gilmore AP, Rowe AJ, Gratzer WB, Critchley DR. 1995. Association of structural repeats in the a-actinin rod domain. Alignment of inter-subunit interactions. *Journal of Molecular Biology* **252**:227–234 DOI 10.1006/jmbi.1995.0490.

Flood G, Rowe AJ, Critchley DR, Gratzer WB. 1997. Further analysis of the role of spectrin repeat motifs in alpha-actinin dimer formation. *European Biophysics Journal* **25**:431–435 DOI 10.1007/s002490050057.

Foley KS, Young PW. 2014. The non-muscle functions of actinins: an update. *Biochemical Journal* **459**:1–13 DOI 10.1042/BJ20131511.

Fujiwara K, Porter ME, Pollard TD. 1978. Alpha-actinin localization in the cleavage furrow during cytokinesis. *Journal of Cell Biology* **79**:268–275 DOI 10.1083/jcb.79.1.268.

Gautel M, Djinovic-Carugo K. 2016. The sarcomeric cytoskeleton: from molecules to motion. *Journal of Experimental Biology* **219**:135–145 DOI 10.1242/jeb.124941.

Geiger B, Avnur Z, Rinnerthaler G, Hinssen H, Small VJ. 1984. Microfilament-organizing centers in areas of cell contact: cytoskeletal interactions during cell attachment and locomotion. *Journal of Cell Biology* **99**:83s–91s DOI 10.1083/jcb.99.1.83s.

Gilson PR, Su V, Slamovits CH, Reith ME, Keeling PJ, McFadden GI. 2006. Complete nucleotide sequence of the chlorarachniophyte nucleomorph: nature's smallest nucleus. *Proceedings of the National Academy of Sciences of the United States of America* **103**:9566–9571 DOI 10.1073/pnas.0600707103.

Gould SB, Waller RF, McFadden GI. 2008. Plastid evolution. *Annual Review of Plant Biology* **59**:491–517 DOI 10.1146/annurev.arplant.59.032607.092915.

Hamill KJ, Hiroyasu S, Colburn ZT, Ventrella RV, Hopkinson SB, Skalli O, Jones JC. 2015. Alpha actinin-1 regulates cell-matrix adhesion organization in keratinocytes: consequences for skin cell motility. *Journal of Investigative Dermatology* **135**:1043–1052 DOI 10.1038/jid.2014.505.

Hasegawa H, Holm L. 2009. Advances and pitfalls of protein structural alignment. *Current Opinion in Strutural Biology* **19**:341–348 DOI 10.1016/j.sbi.2009.04.003.

Kallberg M, Wang H, Wang S, Peng J, Wang Z, Lu H, Xu J. 2012. Template-based protein structure modeling using the RaptorX web server. *Nature Protocols* **7**:1511–1522 DOI 10.1038/nprot.2012.085.

Krabberød AK, Orr RJS, Bråte J, Kristensen T, Bjørklund KR, Shalchian-Tabrizi K. 2017. Single cell transcriptomics, mega-phylogeny, and the genetic basis of morphological innovations in Rhizaria. *Molecular Biology and Evolution* **34**:1557–1573 DOI 10.1093/molbev/msx075.

Kusunoki H, MacDonald RI, Mondragon A. 2004. Structural insights into the stability and flexibility of unusual erythroid spectrin repeats. *Structure* **12**:645–656 DOI 10.1016/j.str.2004.02.022.

Laemmli UK. 1970. Cleavage of structural proteins during the assembly of the head of bacteriophage T4. *Nature* **227**:680–685 DOI 10.1038/227680a0.

Letunic I, Doerks T, Bork P. 2015. SMART: recent updates, new developments and status in 2015. *Nucleic Acids Research* **43**:D257–D260 DOI 10.1093/nar/gku949.

Li Y, Christensen JR, Homa KE, Hocky GM, Fok A, Sees JA, Voth GA, Kovar DR. 2016. The F-actin bundler alpha-actinin Ain1 is tailored for ring assembly and constriction during cytokinesis in fission yeast. *Molecular Biology of the Cell* **27**:1821–1833 DOI 10.1091/mbc.E16-01-0010.

Ma J, Wang S, Zhao F, Xu J. 2013. Protein threading using context-specific alignment potential. *Bioinformatics* **29**:i257–i265 DOI 10.1093/bioinformatics/btt210.

MacDonald RI, Musacchio A, Holmgren RA, Saraste M. 1994. Invariant tryptophan at a shielded site promotes folding of the conformational unit of spectrin. *Proceedings of the National Academy of Sciences of the United States of America* **91**:1299–1303 DOI 10.1073/pnas.91.4.1299.

Maruyama K, Ebashi S. 1965. Alpha-actinin, a new structural protein from striated muscle. II. Action on actin. *Journal of Biochemistry* **58**:13–19 DOI 10.1093/oxfordjournals.jbchem.a128158.

Maruyama K, Mikawa T, Ebashi S. 1984. Detection of calcium binding proteins by ^{45}Ca autoradiography on nitrocellulose membrane after sodium dodecyl sulfate gel electrophoresis. *Journal of Biochemistry* **95**:511–519 DOI 10.1093/oxfordjournals.jbchem.a134633.

Matsudaira P. 1994. Actin crosslinking proteins at the leading edge. *Seminars in Cell and Developmental Biology* **5**:165–174.

McGough A. 1998. F-actin-binding proteins. *Current Opinion in Strutural Biology* **8**:166–176 DOI 10.1016/S0959-440X(98)80034-1.

Meacci G, Wolfenson H, Liu S, Stachowiak MR, Iskratsch T, Mathur A, Ghassemi S, Gauthier N, Tabdanov E, Lohner J, Gondarenko A, Chander AC, Roca-Cusachs P, O'Shaughnessy B, Hone J, Sheetz MP. 2016. alpha-Actinin links extracellular matrix rigidity-sensing contractile units with periodic cell-edge retractions. *Molecular Biology of the Cell* **27**:3471–3479 DOI 10.1091/mbc.E16-02-0107.

Neilson JAD, Rangsrikitphoti P, Durnford DG. 2017. Evolution and regulation of *Bigelowiella natans* light-harvesting antenna system. *Journal of Plant Physiology* DOI 10.1016/j.jplph.2017.05.019.

Otey CA, Carpen O. 2004. α-actinin revisited: a fresh look at an old player. *Cell Motility and the Cytoskeleton* **58**:104–111 DOI 10.1002/cm.20007.

Pantazatos DP, MacDonald RI. 1997. Site-directed mutagenesis of either the highly conserved Trp-22 or the moderately conserved Trp-95 to a large, hydrophobic residue reduces the thermodynamic stability of a spectrin repeating unit. *Journal of Biological Chemistry* **272**:21052–21059 DOI 10.1074/jbc.272.34.21052.

Pardee JD, Spudich JA. 1982. Purification of muscle actin. *Methods in Enzymology* **85 Pt B**:164–181.

Pettersen EF, Goddard TD, Huang CC, Couch GS, Greenblatt DM, Meng EC, Ferrin TE. 2004. UCSF Chimera—a visualization system for exploratory research and analysis. *Journal of Computational Chemistry* **25**:1605–1612 DOI 10.1002/jcc.20084.

Rogers MB, Archibald JM, Field MA, Li C, Striepen B, Keeling PJ. 2004. Plastid-targeting peptides from the chlorarachniophyte *Bigelowiella natans*. *Journal of Eukaryotic Microbiology* **51**:529–535 DOI 10.1111/j.1550-7408.2004.tb00288.x.

Sjöblom B, Salmazo A, Djinovic-Carugo K. 2008. α-actinin structure and regulation. *Cellular and Molecular Life Sciences* **65**:2688–2701 DOI 10.1007/s00018-008-8080-8.

Sobue K, Kanda K. 1989. Alpha-actinins, calspectin (brain spectrin or fodrin), and actin participate in adhesion and movement of growth cones. *Neuron* **3**:311–319 DOI 10.1016/0896-6273(89)90255-9.

Spudich JA, Watt S. 1971. The regulation of rabbit skeletal muscle contraction. Biochemical studies of the interaction of the tropomyosin-troponin complex with actin and the proteolytic fragments of myosin. *Journal of Biological Chemistry* **246**:4866–4871.

Virel A, Addario B, Backman L. 2007. Characterization of Entamoeba histolytica α-actinin2. *Molecular and Biochemical Parasitology* **154**:82–89 DOI 10.1016/j.molbiopara.2007.04.010.

Virel A, Backman L. 2004. Molecular evolution and structure of α-actinin. *Molecular Biology and Evolution* **21**:1024–1031 DOI 10.1093/molbev/msh094.

Virel A, Backman L. 2006. Characterization of Entamoeba histolytica α-actinin. *Molecular and Biochemical Parasitology* **145**:11–17 DOI 10.1016/j.molbiopara.2005.09.003.

Virel A, Backman L. 2007. A comparative and phylogenetic analysis of the α-actinin rod domain. *Molecular Biology and Evolution* **24**:2254–2265 DOI 10.1093/molbev/msm168.

Wachsstock DH, Schwarz WH, Pollard TD. 1993. Affinity of α-actinin for actin determines the structure and mechanical properties of actin filament gels. *Biophysical Journal* **65**:205–214 DOI 10.1016/S0006-3495(93)81059-2.

Wasenius VM, Närvänen O, Lehto VP, Saraste M. 1987. Alpha-actinin and spectrin have common structural domains. *FEBS Letters* **221**:73–76 DOI 10.1016/0014-5793(87)80354-X.

Wehland J, Osborn M, Weber K. 1979. Cell-to-substratum contacts in living cells: a direct correlation between interference-reflexion and indirect-immunofluorescence microscopy using antibodies against actin and alpha-actinin. *Journal of Cell Science* **37**:257–273.

Wilson D, Pethica R, Zhou Y, Talbot C, Vogel C, Madera M, Chothia C, Gough J. 2009. SUPERFAMILY—sophisticated comparative genomics, data mining, visualization and phylogeny. *Nucleic Acids Research* **37**:D380–D386 DOI 10.1093/nar/gkn762.

Winder SJ, Ayscough KR. 2005. Actin-binding proteins. *Journal of Cell Science* **118**:651–654 DOI 10.1242/jcs.01670.